Modeling of a dielectric barrier discharge used as a flowing chemical reactor

Please check the document version of this publication:

Link to publication

Modeling of a dielectric barrier discharge used as a flowing chemical reactor

D. Petrović[1,2], T. Martens[1], J. van Dijk[3], W. J. M. Brok[3], and A. Bogaerts[1]

[1]Research group PLASMANT, Dep. of Chemistry, University of Antwerp, Belgium
[2]Institute of Physics, University of Belgrade, Serbia
[3]Department of Applied Physics, Eindhoven University of Technology, The Netherlands

E-mail: `dragana.petrovic@ua.ac.be`

Abstract. Our aim is to develop and optimize a model for a dielectric barrier discharge used as a chemical reactor for gas treatment. In order to determine the optimum operating conditions, we have studied the influence of the gas flow rate, reactor geometry and applied voltage parameters on the discharge characteristics.

For this purpose, a two-dimensional time-dependent fluid model has been applied to an atmospheric pressure DBD in helium with nitrogen impurities, in a cylindrical geometry. The numerical model is based on the continuity and flux equations for each type of particles treated, the electron energy equation and the Poisson equation. The gas flow is incorporated in the flux equations as a source term. The set of coupled partial differential equations is solved by the so-called modified strongly implicit method. The background gas flow is numerically treated separately, assuming in the model that there is no influence of the plasma on the flow. Indeed, the gas convection velocity is calculated using the commercial code Fluent and it is used as input into the 2D fluid model. The plasma characteristics have been studied in terms of gas flow rate, applied voltage amplitude and frequency, and geometrical effects. The electric currents as a function of time for a given applied potential have been obtained, as well as the number densities and fluxes of plasma species.

1. Introduction

Chemical treatment of gases and liquids, as well as surface treatment, are some of the industrial applications of atmospheric pressure dielectric barrier discharges (DBDs). They are also efficient generators of atoms, free radicals and chemically active species [1]. One of their main advantages is that due to the non-thermal character of DBDs, they operate at room temperature while the electrons are still highly energetic. This enables reactions that thermodynamically would not occur at such low gas temperatures and it can make DBDs efficient plasma-chemical reactors.

The average energy of the electrons generated in DBDs, as well as the discharge characteristics in general, strongly depend on the gap width, the applied frequency, the power input, the type of carrier gas and the type of dielectric used. Our aim is to develop a model for a dielectric barrier discharge used as a flowing chemical reactor for gas treatment. Due to small dimensions of DBD setups, plasma diagnostic studies are not easy and numerical modeling is very important for understanding the discharge behaviour. In the present paper, in order to determine the optimum operating conditions, we discuss some aspects of the influence of the gas flow rate, reactor geometry and applied voltage parameters on the discharge characteristics.

In Section 2 the numerical model and the basic equations are given. A short description of the setup under consideration and the operating conditions is in Section 3. In Section 4, results obtained in the numerical modeling are presented. Finally, conclusions are in Section 5.

2. Numerical model

For this purpose, a two-dimensional time-dependent fluid model for an atmospheric pressure DBD, as a part of the Plasimo code [2], has been applied. It was originally developed by Hagelaar for a DBD used in plasma display panels [3] and later transformed and extended by Brok and van Dijk, and integrated into the Plasimo code [4, 5].

2.1. Basic equations

The model is based on the continuity equations and equations of motion for each type of particles treated:

$$\frac{\partial n_\alpha}{\partial t} + \nabla \vec{\Gamma}_\alpha = S_\alpha, \quad S_\alpha = \sum_j c_{\alpha j} R_{\alpha j}, \quad R_{\alpha j} = k_j n_j n_\alpha, \tag{1}$$

and

$$\vec{\Gamma}_\alpha = \pm \mu_\alpha \vec{E} n_\alpha - D_\alpha \nabla n_\alpha + n_\alpha \vec{v}_b, \tag{2}$$

where the subscript α denotes the type of species. $\vec{v}_b$ is background flow velocity and all the other symbols retain their conventional meaning. Note that the mobility is taken as a positive value for the positive ions and a negative value for the electrons (and negative ions, if included in the model). For the neutral species, the first term in Eq. 2 is zero.

For the electrons an energy-balance equation is also solved:

$$\frac{\partial n_e \bar{\varepsilon}}{\partial t} + \nabla \vec{\Gamma}_{\bar{\varepsilon}} = S_{\bar{\varepsilon}}, \tag{3}$$

where $\bar{\varepsilon}$ is the mean electron energy and $\vec{\Gamma}_{\bar{\varepsilon}}$ is the electron energy flux density given by [6]:

$$\vec{\Gamma}_{\bar{\varepsilon}} = -\frac{5}{3} \mu_e \vec{E} n_e \bar{\varepsilon} - \frac{5}{3} n_e D_e \nabla \bar{\varepsilon}. \tag{4}$$

Note that the energy changes are usually a loss of energy (i.e. ionization and excitation) but a gain of energy can occur as well as a result of superelastic collisions. For the ions and neutral species no energy-balance equation needs to be included, because these species can be regarded as being at the same energy (temperature) as the background gas. The gas temperature is assumed to be 300 K, uniformly distributed over the discharge. Moreover, for these species, the local field approximation can be used, i.e. the mobility and diffusion coefficients of the heavy particles are taken to be functions of the local reduced electric field (local field divided by pressure). The values used are taken from Ref. [7].

In order to obtain a self consistent electric field distribution the Poisson equation:

$$\epsilon \nabla \vec{E} = \sum_\alpha q_\alpha n_\alpha, \tag{5}$$

is solved as well, not only within the plasma but also inside the dielectrics, where it is reduced to $\epsilon \nabla \vec{E} = 0$ because no species are present inside the dielectrics.

2.2. Gas flow

The gas flow is incorporated in the flux equations as a source term (the third term on the right side of Eq. 2) [8]. The fundamental assumption in the model is that the plasma does not influence the flow. This allows us a separate numerical treatment of the background gas flow and use the results as input for the plasma calculation.

On the other hand, the flow influences the plasma as a momentum source for the species. This momentum source enters in the drift-diffusion equations. This effect is particularly important for the neutral species, as there are no electric forces to modify their speed.

The gas convection velocity is calculated using the commercial computational fluid dynamics code Fluent [9], i.e., by solving the conservation equations for mass, momentum and energy. The solution was considered to converge when the residuals of the guiding equations have become smaller than 10^{-6}.

2.3. Modeling chemistry

The model is applied here to a DBD in helium with 100 ppm nitrogen impurity. The species included in the model are the background gases He and N_2, electrons, He^+, He_2^+, N_2^+ and N_4^+ ions, He_2 excimer, and He atoms excited to the metastable levels.

For most of the electron-induced processes the reaction rates are calculated on the basis of energy-dependent cross-sections, and with a separate program, called BOLSIG+, which is based on a Boltzman equation [10]. This program is applied for a wide range of different, fixed reduced electric fields. For each value of the reduced electric field the average electron energy, the mobility of the electrons, and the rates of the different electron-induced processes are tabulated. By use of these tables, the rates, mobilities, and diffusion coefficients (derived from the mobilities using the well-known Einstein relationship, assuming the bulk electrons are Maxwellian), will be applied corresponding to the electron energy calculated with the above electron-energy-balance equation. Details about the chemistry model and the reactions taken into account can be found in [11]-[13].

The effect of charge accumulation on the dielectric materials is also considered. The boundary conditions of the electrons are largely determined by secondary electron emission from the ions. Following the procedure of Hagelaar et al. [14] we use a constant secondary-electron emission coefficient of 0.05 for the helium ions and 0.001 for nitrogen ions and also consider that this ion-induced secondary-electron emission produces electrons with a mean initial energy of 4 eV. Reflection at the walls is neglected and electron desorption from the dielectrics is not considered, because it has been stated [15] that the latter process is very unlikely to happen.

The equations (1)-(5) are solved within the same time-step by the so-called modified strongly implicit method, developed by Schneider and Zedan [16], and using an extra stabilization method, as explained elsewhere [3], until convergence is reached within every time-step of the periodic cycle, and periodic behaviour over the discharge cycles is obtained.

3. Setup and conditions

The model was applied to a cylindrical DBD reactor consisting of two coaxial stainless steel electrodes with 2 mm thick alumina as a dielectric on the inner side of the outer electrode, as illustrated schematically in Fig. 1. The gap width is varied from 0.7 mm over 1.5 mm to 3 mm by changing the diameter of the inner tube. The length of the reactor is kept fixed at 9 cm and the outer diameter is 3 cm. A sine shaped high voltage is applied on the inner electrode whereas the other electrode was grounded. As it is already mentioned, we applied the model to a helium DBD with nitrogen impurity at atmospheric pressure and temperature 300 K.
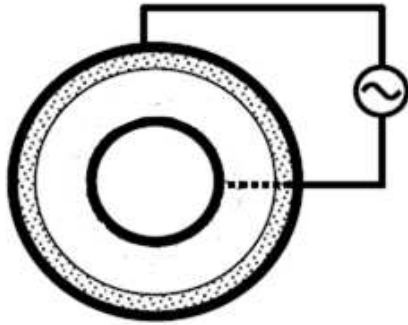
Figure 1. Schematic diagram of the setup.

4. Results

4.1. Discharge characteristics

The plasma characteristics have been studied in terms of applied voltage amplitude and frequency, and geometrical effects. The influence of the gap width on the electron number density is shown in Fig. 2. It can be seen that at 20 kHz and 20 kV applied voltage a decrease of the gap width leads to an increase of the electron number density in the system (see Fig. 2a), as has been experimentally observed as well [17]-[19]. The highly energetic electrons will lead to the generation of some highly active species including radicals that is very desirable for the purpose of a chemical reactor for gas conversion. However, applying different voltage characteristics (i.e., voltage amplitude and frequency) this regular behaviour can change, as can be seen in Fig. 2b. In this particular case, when the applied voltage frequency and amplitude are 75 kHz and 10 kV, respectively, the highest electron number density is for 1.5 mm gap distance.
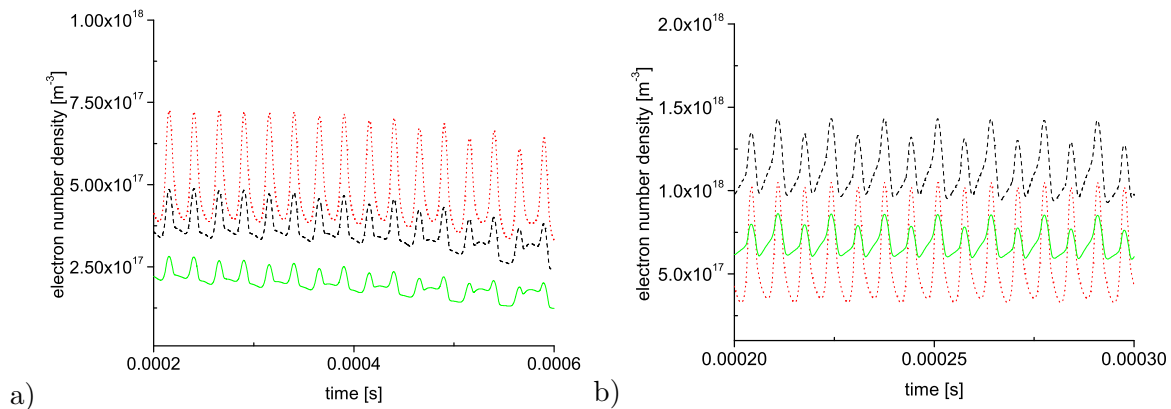

Figure 2. Calculated spatially averaged electron number density as a function of time, for the gap width 0.7 mm - red dotted line, 1.5 mm - black dashed line, and 3 mm - green solid line. The applied voltage frequency and amplitude are a) 20 kHz, 20 kV; b) 75 kHz, 10 kV.

The spatially averaged total electric currents as a function of time for different values of applied potential amplitude and frequency are shown in Fig. 3. A clear transition from one narrow peak, over multipeak to a broad profile can be seen. The total current consists of discharge and displacement currents and when the discharge component is dominant narrow peaks will appear (see Fig. 3a) that is usually reported in the literature [20]-[23]. Increase of the voltage amplitude might cause a multibreakdown in the system and produce a multipeak current profile (see Fig. 3b). On the other hand, increase of the applied frequency leads to an increase of the displacement current and broadening of the current peaks. In Fig. 3c a clear superposition of the displacement current (sine shaped profiles) and the discharge current (narrow peaks) is seen.
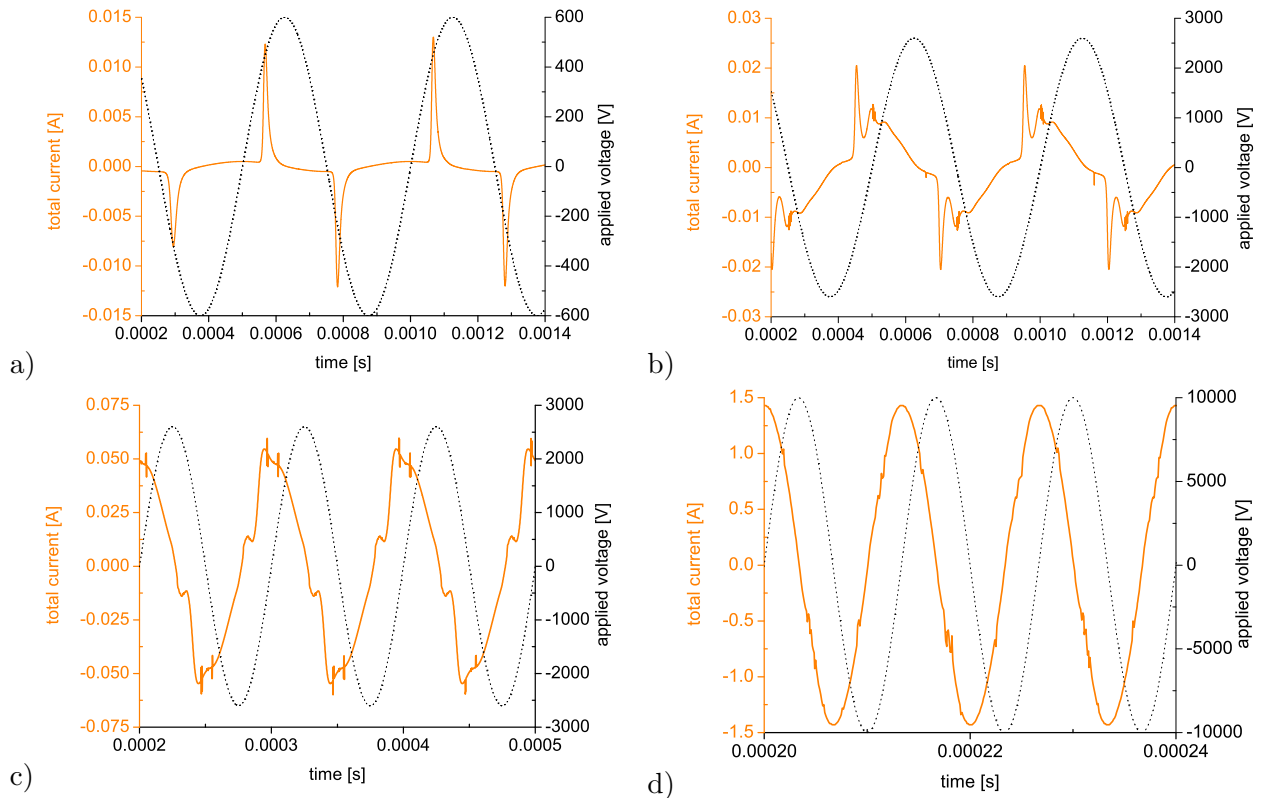
Figure 3. Calculated total currents (orange solid lines) as a function of time in an atmospheric DBD in helium with 100 ppm nitrogen impurity, for different applied voltage frequencies and amplitudes: a) 2 kHz, 0.6 kV; b) 2 kHz, 2.6 kV; c) 10 kHz, 2.6 kV; d) 75 kHz, 10 kV (black dotted lines). The gap width is 0.7 mm.

Further increase of the applied voltage frequency and amplitude will cause that the displacement current becomes dominant and the total current profile becomes very broad, with an almost sine shaped profile (see Fig. 3d).

4.2. Gas flow effect

The adjustment of flow rate allows the creation of uniform DBDs with optimized input power while a lower breakdown electric field is required [24]. Transition from a streamer discharge to a silent glow discharge due to the presence of a flow in the system is also reported in Ref. [25]. An increase of species fluxes (except for the electrons) due to convection in a Grimm-type glow discharge is shown in Ref. [26]. For gas conversion applications it has been observed that the increase of the gas flow rate reduces the conversion and decreases the yields. On the other hand, the effect of the flow rate on product selectivity depends on the particle type [27]-[29].

As it is already mentioned, the gas convection velocity was calculated using the Fluent code [9]. The feed gas is usually introduced into the reactor via a mass flow controller. Because of this, the mass flow at the reactor inlet was given as a boundary condition in the background gas flow velocity calculations. The flow was considered to be laminar and a steady state was assumed.

For a mass flow rate of 5 l/min, the calculated axial velocity profile at z=4.5 cm, as a function of radial position (i.e., in the gap between both concentric electrodes), is shown in Fig. 4. The flow velocity reaches a maximum (around 2.2 m/s) in the middle of the gap. At the walls,

the flow velocity becomes zero due to the viscous drag. The radial component of the velocity is calculated to be negligible compared to the axial one and it is taken to be zero in further calculations. A two dimensional velocity profile in the total reactor (axial symmetry is assumed) and a zoomed in profile are shown in Fig. 5.
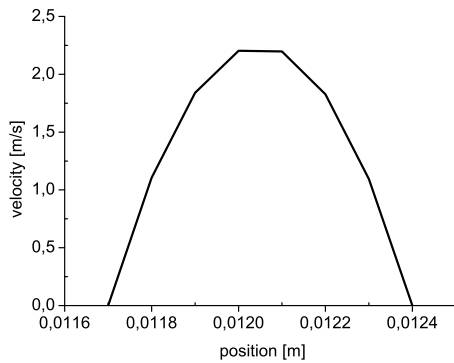

Figure 4. Axial velocity profile at z=4.5 cm, as a function of radial position, for a mass flow rate of 5 l/min.

The calculated background gas convection velocity is used as input in the 2D fluid model. The radial and axial flux of the He_2 species with gas flow in the system at the maximum gas velocity (r=0.0121 cm, z=4.5 cm) are shown in Fig. 6a and Fig. 6b, respectively. The radial flux of the He_2 species without gas flow at the same position is shown in Fig. 7a. As can be seen (compare Fig. 6a and Fig. 7a), there is no influence of the convection on the flux in the radial direction, which is expected since the radial component of the gas flow is negligible. On the other hand, without gas flow in the system, there was no flux of He_2 species in the axial direction. However,
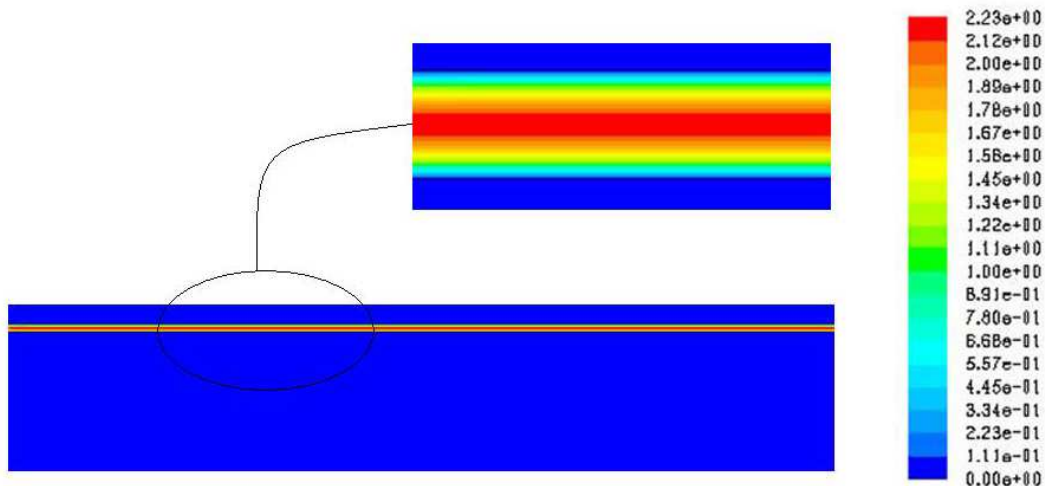

Figure 5. Contours of velocity magnitude (in [m/s]) in the total reactor and zoomed in view of the gap. The mass flow rate is 5 l/min. The gap width is 0.7 mm, the length is 9 cm, the diameters of outer and inner electrode are 30 mm and 24.6 mm, respectively, and the dielectric thickness is 2mm.

introduction of a flow of 5 l/min gives rise to an axial flux, which is one order of magnitude higher than the radial one (see Fig. 6b). A similar influence of the gas flow can be observed on
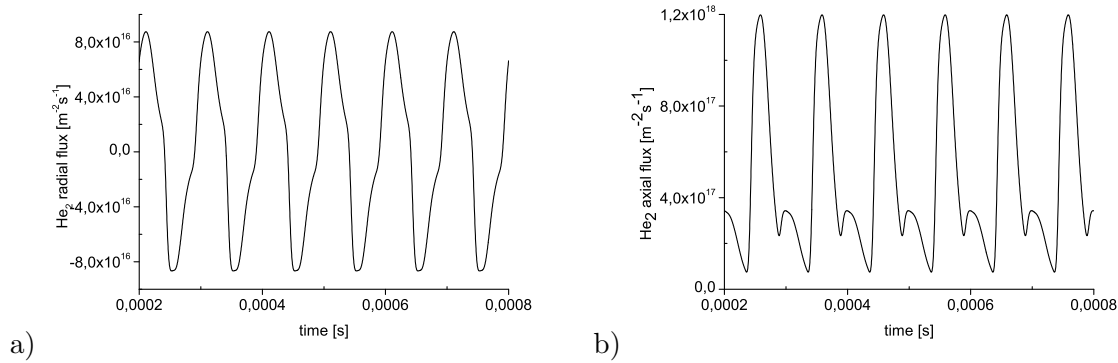

Figure 6. Calculated a) radial and b) axial fluxes of He_2 for a mass flow rate of 5 l/min. The applied voltage frequency and amplitude are 10 kHz and 2.6 kV. The gap width is 0.7 mm.

the ion fluxes, Fig. 8. While the radial flux remains unchanged, the axial flux appears in the system. However, opposite to the case of neutrals where the axial flux becomes dominant due to the flow, for the ions it remains two - three orders of magnitude lower than the radial flux. Indeed, as can be seen from these figures, the axial flux is of the order of 10^{16}, 10^{17} $\mathrm{m^{-2}s^{-1}}$ (see Fig. 8) while the radial flux is of the order of 10^{19} $\mathrm{m^{-2}s^{-1}}$ (see Fig. 7b).
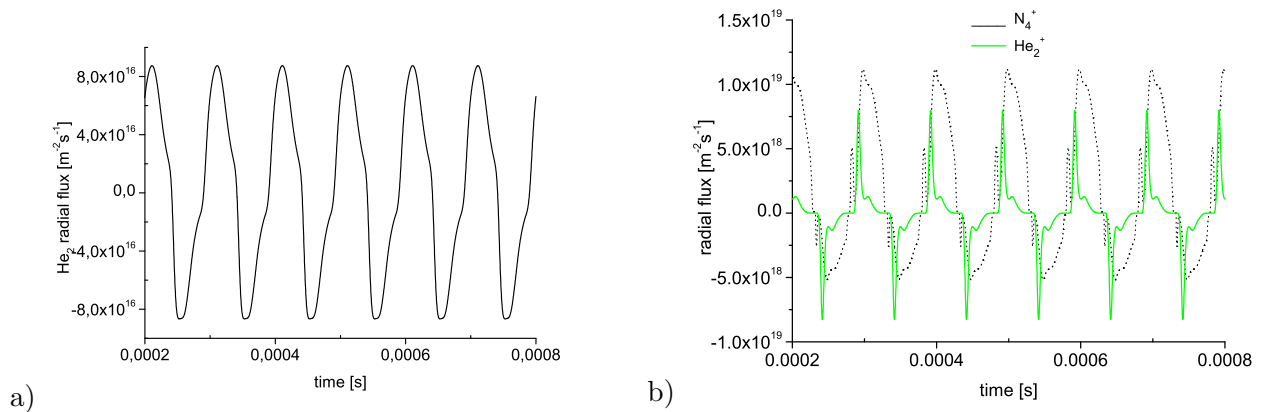

Figure 7. Calculated radial fluxes of a) He_2 and b) He_2^+ (green solid line) and N_4^+ (black dotted line) without gas flow. The applied voltage frequency and amplitude are 10 kHz and 2.6 kV. The gap width is 0.7 mm.

5. Conclusions

We have presented the influence of the gas flow rate, reactor geometry and applied voltage parameters on the discharge characteristics of a cylindrical DBD in helium with nitrogen impurity. This study shows that discharge voltage and frequency effects have a large impact on the electric current profiles, which can range from one narrow peak, over multipeak to a broad profile. A decrease of the gap width leads to an increase of the electron number density, while applying a higher voltage frequency can change this regular behaviour. A gas flow rate in the system causes appearance of the axial fluxes of neutral species, as well as of ions, while the radial fluxes remain unchanged.
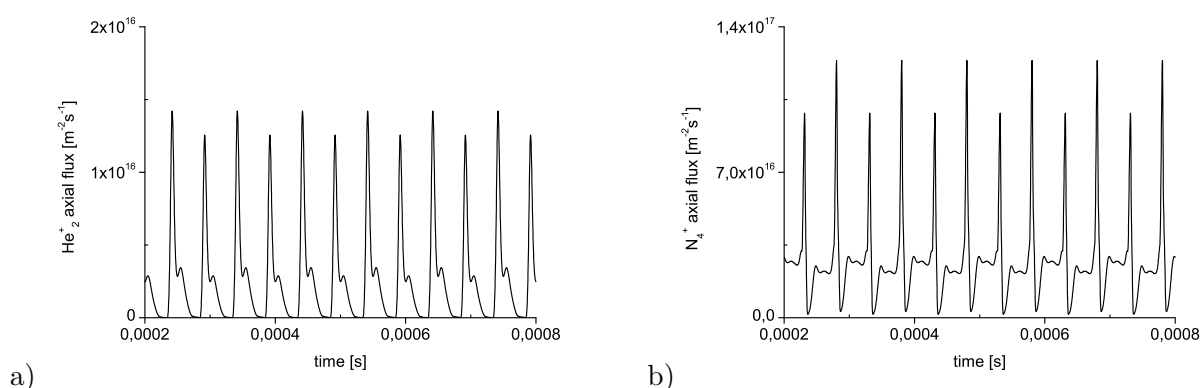
Figure 8. Calculated axial fluxes of a) He_2^+ and b) N_4^+ for a mass flow rate of 5 l/min. The applied voltage frequency and amplitude are 10 kHz and 2.6 kV. The gap width is 0.7 mm.

References

[1] Kogelschatz U 2003 *Plasma Chemistry And Plasma Processing* **23**(1) 1
[2] http://plasimo.phys.tue.nl
[3] Hagelaar G 2000 *Modeling of Microdischarges for Display Technology*, PhD Dissertation, Eindhoven University of Technology
[4] Brok WJM, van Dijk J, Bowden MD, van der Mullen JJAM, Kroesen GMW 2003 *J Phys D: Appl Phys* **36** 19671979
[5] Brok WJM, Gendre MF, van der Mullen JJAM 2006 *J Phys D: Appl Phys* **40** 156162
[6] Raizer YP 1991 *Gas discharge physics* Springer, Berlin Heidelberg New York
[7] Ellis HW, Pai RY, McDaniel EW 1976 *At Data Nucl Data Tables* **17** 177210
[8] Broks BHP, Brok WJM, Remy J, van der Mullen JJAM, Benidar A, Biennier L, and Salama F 2005, *Phys. Rev. E* **71**(3), 036409.
[9] http://www.fluent.com
[10] Hagelaar GJM, Pitchford LC 2005 *Plasma Sources Sci Technol* **14** 722733
[11] Martens T, Bogaerts A, Brok W, van Dijk J 2007 *Anal. Bioanal. Chem.* **388** 1583
[12] Martens T, Bogaerts A, Brok WJM, van der Mullen JJAM 2007 *J. Anal. At. Spectrom.* **22** 1033
[13] Martens T, Bogaerts A, Brok W, van Dijk J 2008 *Appl. Phys. Lett.* **92** 041504
[14] Hagelaar GJM, Kroesen GMW, van Slooten U, Schreuders H (2000) *J Appl Phys* **88** 22522262
[15] Raizer YP, Shneider MN, Yatsenko NA 1995 *Radio-frequency capacitive discharges* CRC Press, Florida
[16] Schneider GE, Zedan M 1981 *Numer Heat Transfer* **4** 119
[17] Kogelschatz U, Eliasson B 1995 *Handbook of Electrostatic Processes*, Marcel Dekker, New York 581
[18] Kogelschatz U, Eliasson B 1997 *J. Phys. IV*, **7** 46
[19] Eliasson B, Kogelschatz U 1991 *IEEE Trans. Plasma Sci.* **19** 309
[20] Golubovskii YuB, Maiorov VA, Behnke J., and Behnke VG 2002 *J. Phys. D: Appl. Phys.* **36**
[21] Mangolini L, Anderson C, Heberlein J, and Kortshagen 2004 *J. Phys. D: Appl. Phys.* **36** 1021
[22] Massines F, Rabehi A, Decomps P, and Gardi RB. 1998 *J. Appl. Phys.* **83** 2950
[23] Wang Y-H and Wang D-Z. 2004 *Chin. Phys. Lett.* **21** 2234
[24] Nersisyan G, Graham WG 2004 *Plasma Sources Sci. Technol.* **13** 582
[25] Gherardi N, Massines F 2001 *IEEE Trans. Plasma Sci.* **29** 536
[26] Bogaerts A, Okhrimovskyy, R. Gijbels 2002 *J. Anal. At. Spectrom.* **17** 1076
[27] Pietruszka B, Anklam K, Heintze M 2004 *Appl. Catal. A: General* **261** 19
[28] Song HK, Choi JW, Yue SH, Lee H, Na BK 2004 *Catalysis Today* **89** 27
[29] Jian T, Li Y, Liu Ch, Xu G, Eliasson B, Xue B 2002 *Catalysis Today* **72** 229